EXPERIMENTAL AND THEORETICAL ANALYSIS OF TRANSIENT CONJUGATED CONDUCTION - EXTERNAL CONVECTION

Mohammed Lachi, m.lachi@univ-reims.fr
Laboratoire de Thermomécanique – LTM
Université de Reims, France

Carolina Palma Naveira, cpnaveira@yahoo.com.br
LTTC – Laboratory of Transmission and Technology of Heat
Mechanical Engineering Department – POLI/COPPE, Universidade Federal do Rio de Janeiro, UFRJ
Cx. Postal 68503 – Cidade Universitária, 21945-970, Rio de Janeiro, RJ, Brasil.

Mourad Rebay, mourad.rebay@univ-reims.fr
Laboratoire de Thermomécanique – LTM
Université de Reims, France

Renato Machado Cotta, cotta@mecanica.coppe.ufrj.br
LTTC – Laboratory of Transmission and Technology of Heat
Mechanical Engineering Department – POLI/COPPE, Universidade Federal do Rio de Janeiro, UFRJ
Cx. Postal 68503 – Cidade Universitária, 21945-970, Rio de Janeiro, RJ, Brasil.

Abstract. *This work presents a critical comparison of experimental results and hybrid numerical-analytical solutions for transient laminar forced convection over flat plates of non-negligible thickness, subjected to time variations of the applied wall heat flux at the interface fluid-solid wall. This conjugated conduction-convection problem is first simplified through the employment of the Coupled Integral Equations Approach (CIEA) to reformulate the heat conduction problem on the plate by averaging the related energy equation in the transversal direction. As a result, a partial differential formulation for the transversally averaged wall temperature is obtained, and rewriting the boundary condition for the fluid in the heat balance at the solid-fluid interface. From available velocity distributions, the solution method is then proposed for the coupled partial differential equations within the thermal boundary layer, based on the Generalized Integral Transform Technique (GITT) under its partial transformation mode, combined with the method of lines implemented in the Mathematica 5.2 routine NDSolve. For the experimental results, an apparatus was employed involving an air blower to cool and flash lamps to heat a vertical PVC plate of 33 cm in length and 12 mm in thickness, while the exposed surface temperature is measured by infrared thermography. Fluxmeter and thermocouple measurements are also utilized to covalidate the infrared camera measurements and to provide estimates of heat losses. The transient evolution of the measured surface temperatures along the plate length are critically compared against the simulation results, and the model is then analyzed to illustrate the major effects that require further treatment for a closer agreement with the experimental findings.*

Keywords*: Forced convection, Conjugated Problem, Infrared Thermography, Hybrid Methods, Integral Transforms*

1. INTRODUCTION

The analysis of conjugated convection-conduction heat transfer problems has been challenging thermal sciences researchers along the last few decades, since the pioneering work of (Perelman, 1961) and (Luikov et al., 1971; Luikov, 1974). In engineering practice, most conjugated problems are handled in an iterative manner, by successively solving the convection and conduction problems, or just by fully neglecting the coupling between the two phenomena when accuracy is not at a premium. On the other hand, advanced design methodologies nowadays benefit from widely available automatic software for computational fluid mechanics and heat transfer, based on classical discrete numerical approaches (Minkowycz et al., 2006). Nevertheless, it remains of interest to provide more accurate approaches and, at the same time less computationally intensive, to this class of problems, which frequently appear in thermal engineering applications. Hybrid numerical-analytical approaches are particularly well-suited in providing solutions to conjugated problems, which may lead to both accuracy improvement with respect to the simplified engineering approaches and reduced computational involvement in comparison to purely numerical methods, as illustrated within a number of contributions (Guedes et al., 1991; Vynnycky et al., 1998; Mossad, 1999; Pozzi & Tognaccini, 2000; Lachi et al., 2003). One such hybrid approach that has been previously employed in the solution of conjugated problems is known as the Generalized Integral Transform Technique (GITT), belonging to a class of methods that combine eigenfunction expansions with the numerical solution of transformed ordinary differential systems (Cotta, 1993; Cotta & Mikhailov, 1997; Cotta, 1998, Santos et al., 2001; Cotta & Mikhailov, 2006).

In addition, the analysis of transient forced convection problems has renewed the interest on conjugation effects interpretation, in light of the marked influence of both thermal capacitance and resistance of the solid walls on the flowing fluid thermal behavior (Cotta et al., 1987; Guedes & Cotta, 1991; Guedes et al., 1994; Lachi et al., 2006). A number of mixed experimental and theoretical works have also been reported in an attempt to quantify and covalidate the convective behavior under such transient conjugated conditions (Remy et al., 1995; Rebay et al., 2002; Rebay et al., 2008). Also quite recently, a hybrid solution again based on the Generalized Integral Transform Technique has been proposed to transient conjugated conduction-external convection problems, (Naveira et al., 2007; Naveira et al., 2008), which provided important physical interpretation of the heat flux transient partition between the solid and the fluid for an imposed heat flux at the solid-fluid interface. The next step is thus the critical comparison of experimental and theoretical results for such transient conjugated situation, in an attempt to validate the modeling and hybrid solution methodology for this class of problems. For this purpose, a more general formulation than the one proposed in (Naveira et al., 2008) is here considered, and the experimental apparatus described in (Rebay et al, 2008) is employed in acquiring the transient thermal behavior of a laminar air flow over a PVC plate heated with flash lamps. Experiments and simulations are then critically compared so as to investigate the different aspects to be improved in either the modeling or the experimental procedure, towards a more perfect matching between the two prediction approaches.

2. THEORETICAL ANALYSIS

The problem here analyzed is a more general version of that proposed by (Naveira et al., 2007; Naveira et al., 2008), so as to adequate the formulation to the experimental conditions, later to be discussed. It involves laminar incompressible flow of a Newtonian fluid over a flat plate, with steady-state flow but transient convective heat transfer due to a time and space variable applied heat flux, $\phi(x^*,t)$, at the solid-fluid interface. The fluid flows with a free stream velocity u_∞, which arrives at the plate front edge at the temperature $T_\infty(t)$, which may vary along the process. The wall is considered to participate on the heat transfer problem, with thickness, e, and length, L. The boundary layer equations are assumed to be valid for the flow and heat transfer problem within the fluid. Thus, the energy equations for the fluid and for the solid are given by:

$$\frac{\partial T_\mathrm{f}(x^*,y^*,t)}{\partial t}+u\frac{\partial T_\mathrm{f}(x^*,y^*,t)}{\partial x^*}+v\frac{\partial T_\mathrm{f}(x^*,y^*,t)}{\partial y^*}=\alpha_\mathrm{f}\frac{\partial^2 T_\mathrm{f}(x^*,y^*,t)}{\partial y^{*2}} \quad , \qquad 0<y^*<\delta_\mathrm{t}^*(x^*,t)\,,\,0<x^*<L\,,\,t>0 \tag{1a}$$

$$\frac{\partial T_\mathrm{s}(x^*,y^*,t)}{\partial t}=\alpha_\mathrm{s}\left(\frac{\partial^2 T_\mathrm{s}(x^*,y^*,t)}{\partial x^{*2}}+\frac{\partial^2 T_\mathrm{s}(x^*,y^*,t)}{\partial y^{*2}}\right) \quad , \quad -e<y^*<0,\,0<x^*<L\,,\,t>0 \tag{1b}$$

with initial, boundary and interface conditions

$$T_\mathrm{f}(x^*,y^*,0)=T_\infty(0)\,, \quad 0<y^*<\infty\,,\,0<x^*<L \tag{1c}$$

$$T_\mathrm{s}(x^*,y^*,0)=T_\infty(0)\,, \quad -e<y^*<0\,,\,0<x^*<L \tag{1d}$$

$$T_\mathrm{f}(x^*,\delta_\mathrm{t}^*,t)=T_\infty(t)\ , \qquad 0<x^*<L\,,\,t>0 \tag{1e}$$

$$T_\mathrm{f}(x^*,0,t)=T_\mathrm{s}(x^*,0,t)\ , \qquad 0<x^*<L\,,\,t>0 \tag{1f}$$

$$-k_\mathrm{f}\left.\frac{\partial T_\mathrm{f}}{\partial y^*}\right|_{y^*=0}=-k_\mathrm{s}\left.\frac{\partial T_\mathrm{s}}{\partial y^*}\right|_{y^*=0}+\phi(x^*,t) \quad , \quad 0<x^*<L\,,\,t>0 \tag{1g}$$

$$-k_\mathrm{s}\left.\frac{\partial T_\mathrm{s}}{\partial y^*}\right|_{y^*=-e}=h_e(T_\infty(t)-T_s) \quad , \quad 0<x^*<L\,,\,t>0 \tag{1h}$$

$$T_\mathrm{f}(0,y^*,t)=T_\infty(t)\ , \qquad 0<y^*<\infty\,,\,t>0 \tag{1i}$$

$$-k_\mathrm{s}\left.\frac{\partial T_\mathrm{s}}{\partial x^*}\right|_{x^*=0}=h_0(T_\infty(t)-T_s) \quad , \quad -e<y^*<0\,,\,t>0 \tag{1j}$$

$$k_\mathrm{s}\left.\frac{\partial T_\mathrm{s}}{\partial x^*}\right|_{x^*=L}=h_L(T_\infty(t)-T_s) \quad , \quad -e<y^*<0\,,\,t>0 \tag{1k}$$

As compared to the analysis in (Naveira et al., 2008), the proposed problem, eqs.(1), incorporates the possibility of heat losses through all the solid boundaries that are not in direct contact with the flowing stream, through the specification of heat transfer coefficients at the boundary conditions (1h, 1j, and 1k), besides the time varying free stream temperature and space and time variable prescribed interface heat flux.

The formulation is now simplified through the proposition of a lumped formulation for the wall, integrating its temperature field along the transversal direction, y^*. Instead of employing the Classical Lumped System Analysis, which essentially assumes the wall temperature field to be uniform in the transversal direction, an improved model is proposed obtained via the coupled integral equations approach (C.I.E.A.) (Cotta & Mikhailov, 1998), based on Hermitetype approximations for integrals. We consider just the two approximations, $H_{0,0}$ and $H_{1,1}$, which correspond, respectively, to the well-known trapezoidal and corrected trapezoidal integration rules, given by:

$$H_{0,0} \rightarrow \int_0^h y(x)\mathrm{d}x \cong \frac{h}{2}\left(y(0)+y(h)\right) \tag{2a}$$

$$H_{1,1} \rightarrow \int_0^h y(x)\mathrm{d}x \cong \frac{h}{2}\left(y(0)+y(h)\right)+\frac{h^2}{12}\left(y'(0)-y'(h)\right) \tag{2b}$$

The transversally averaged wall temperature is then approximated by taking the $H_{1,1}$ approximation, the corrected trapezoidal rule. In addition, the transversally averaged wall heat flux is approximated by $H_{0,0}$ approximation, the trapezoidal rule. This $H_{1,1}/H_{0,0}$ combined solution does not change the nature of the problem in comparison with the classical lumped formulation, but only modifies the equation coefficients. Also, it has been shown to be significantly more accurate than the classical lumped system analysis in the applicable range of the governing parameters (Cotta & Mikhailov, 1998).
The transversally averaged wall temperature, $T_{\mathrm{av}}(x^*,t)$, is thus approximated as:

$$T_{\mathrm{av}}(x^*,t) \equiv \frac{1}{e}\int_{-e}^{0} T_{\mathrm{s}}(x^*,y^*,t)dy^* \approx \frac{1}{2}\left[T_{\mathrm{s}}(x^*,0,t)+T_{\mathrm{s}}(x^*,-e,t)\right]+\frac{e}{12}\left[\left.\frac{\partial T_{\mathrm{s}}}{\partial y^*}\right|_{y^*=-e}-\left.\frac{\partial T_{\mathrm{s}}}{\partial y^*}\right|_{y^*=0}\right] \tag{3a}$$

The average heat flux is approximated as:

$$\frac{k_s}{e}\int_{-e}^{0}\frac{\partial T_{\mathrm{s}}(x^*,y^*,t)}{\partial y^*}dy^* \equiv \frac{k_s}{e}\left[T_{\mathrm{s}}(x^*,0,t)-T_{\mathrm{s}}(x^*,-e,t)\right] \approx \frac{k_s}{e}\frac{e}{2}\left[\left.\frac{\partial T_{\mathrm{s}}}{\partial y^*}\right|_{y^*=-e}+\left.\frac{\partial T_{\mathrm{s}}}{\partial y^*}\right|_{y^*=0}\right] \tag{3b}$$

An expression for the temperature at $y^*=-e$, is thus obtained from eq.(3a):

$$T_{\mathrm{s}}(x^*,-e,t)=\frac{ek_s\left.\frac{\partial T_{\mathrm{s}}}{\partial y^*}\right|_{y^*=0}+12k_sT_{\mathrm{av}}(x^*,t)-6k_sT_{\mathrm{s}}(x^*,0,t)+eh_eT_\infty(t)}{eh_e+6k_s} \tag{4a}$$

This expression is substituted into the average heat flux expression, eq.(3b), providing:

$$\left.\frac{\partial T_{\mathrm{s}}}{\partial y^*}\right|_{y^*=0}=\frac{2\left[6k_s\left(T_{\mathrm{s}}(x^*,0,t)-T_{\mathrm{av}}(x^*,t)\right)+eh_e\left(2T_{\mathrm{s}}(x^*,0,t)+T_\infty(t)-3T_{\mathrm{av}}(x^*,t)\right)\right]}{e(eh_e+4k_s)} \tag{4b}$$

For no heat losses at the back face of the plate, i.e., h_e=0, as shown in (Naveira et al., 2008) the above relation is reduced to:

$$\left.\frac{\partial T_{\mathrm{s}}}{\partial y^*}\right|_{y^*=0}=\frac{3}{e}\left[T_{\mathrm{f}}(x^*,0,t)-T_{\mathrm{av}}(x^*,t)\right] \tag{4c}$$

The interface condition (1g) is then written as:

$$-k_{\mathrm{f}}\left.\frac{\partial T_{\mathrm{f}}}{\partial y^*}\right|_{y^*=0}=-k_{\mathrm{s}}\frac{2\left[6k_s\left(T_{\mathrm{f}}(x^*,0,t)-T_{\mathrm{av}}(x^*,t)\right)+eh_e\left(2T_{\mathrm{f}}(x^*,0,t)+T_\infty(t)-3T_{\mathrm{av}}(x^*,t)\right)\right]}{e(eh_e+4k_s)}+\phi(x^*,t) \tag{4d}$$

The energy equation for the solid is now reformulated by taking the average on the transversal direction, operating with $\frac{1}{e}\int_{-e}^{0}\_\_\_dy^*$, to yield:

$$\frac{\partial T_{\mathrm{av}}(x^*,t)}{\partial t} = \alpha_{\mathrm{s}} \frac{\partial^2 T_{\mathrm{av}}(x^*,t)}{\partial x^{*2}} + \frac{\alpha_{\mathrm{s}}}{e} \int_{-e}^{0} \frac{\partial^2 T_{\mathrm{s}}(x^*,y^*,t)}{\partial y^{*2}} dy^*$$
$$= \alpha_{\mathrm{s}} \frac{\partial^2 T_{\mathrm{av}}(x^*,t)}{\partial x^{*2}} + \frac{\alpha_{\mathrm{s}}}{e} \left[\left. \frac{\partial T_{\mathrm{s}}(x^*,y^*,t)}{\partial y^*} \right|_{y^*=0} - \left. \frac{\partial T_{\mathrm{s}}(x^*,y^*,t)}{\partial y^*} \right|_{y^*=-e} \right] \tag{5}$$

We can then eliminate the derivatives at $y^*=0$ and at $y^*=-e$ by applying the boundary condition eq.(1h), and the developed expressions (4a,b), to find:

$$\frac{\partial T_{\mathrm{av}}(x^*,t)}{\partial t} = \alpha_{\mathrm{s}} \frac{\partial^2 T_{\mathrm{av}}(x^*,t)}{\partial x^{*2}} - \frac{6\alpha_s \left[2k_s \left(T_{\mathrm{av}}(x^*,t) - T_{\mathrm{f}}(x^*,0,t) \right) + e h_e \left(2T_{\mathrm{av}}(x^*,t) - T_\infty(t) - T_{\mathrm{f}}(x^*,0,t) \right) \right]}{e^2 (e h_e + 4k_s)} \tag{6a}$$

Again, for no heat losses at the back face of the plate, i.e., h_e=0, the above reformulated energy equation simplifies to:

$$\frac{\partial T_{\mathrm{av}}(x^*,t)}{\partial t} = \alpha_{\mathrm{s}} \frac{\partial^2 T_{\mathrm{av}}(x^*,t)}{\partial x^{*2}} - \frac{3\alpha_{\mathrm{s}}}{e^2} \left[T_{\mathrm{av}}(x^*,t) - T_{\mathrm{f}}(x^*,0,t) \right] \tag{6b}$$

This lumped-differential equation is complemented by the also averaged initial and boundary conditions:

$$T_{\mathrm{av}}(x^*,0) = T_\infty(0) \tag{6c}$$

$$-k_{\mathrm{s}} \left. \frac{\partial T_{\mathrm{av}}(x^*,t)}{\partial x^*} \right|_{x^*=0} = h_0 (T_\infty(t) - T_{\mathrm{av}}(0,t)); \qquad k_{\mathrm{s}} \left. \frac{\partial T_{\mathrm{av}}(x^*,t)}{\partial x^*} \right|_{x^*=L} = h_L (T_\infty(t) - T_{\mathrm{av}}(L,t)) \tag{6d,e}$$

The conjugated conduction-convection problem can also be rewritten after introducing dimensionless variables:

$$U = \frac{u}{u_\infty}, \quad V = \frac{v}{u_\infty}, \qquad x = \frac{x^*}{L}, \quad y = \frac{y^*}{L}, \quad \tau = \frac{u_\infty . t}{L}, \quad \theta = \frac{T - T_\infty(0)}{\frac{\phi_{\mathrm{ref}} . L}{k_{\mathrm{f}}}},$$

$$\theta_\infty(\tau) = \frac{T_\infty(t) - T_\infty(0)}{\frac{\phi_{\mathrm{ref}} . L}{k_{\mathrm{f}}}}, \quad Re_{\mathrm{L}} = \frac{u_\infty . L}{\nu}, \quad Pe_{\mathrm{f}} = \frac{u_\infty . L}{\alpha_{\mathrm{f}}}, \quad Pe_{\mathrm{s}} = \frac{u_\infty . e}{\alpha_s}, \quad \delta_{\mathrm{t}} = \frac{\delta_{\mathrm{t}}^*}{L}, \tag{7}$$

$$Q_{\mathrm{w}} = \frac{\phi}{\phi_{\mathrm{ref}}}, \quad R = \frac{e}{L}, \quad \mathrm{K} = \frac{k_{\mathrm{f}}}{k_{\mathrm{s}}}, \quad Bi_e = \frac{h_e . e}{k_s}, \quad Bi_0 = \frac{h_0 . L}{k_s}, \quad Bi_L = \frac{h_L . L}{k_s}$$

The flow problem solution is considered known, by any chosen approximate analytical or numerical solution technique. The thermal problem is essentially confined to a region here represented by the steady thickness $\delta_{\mathrm{t}}(x)$, which just needs to be large enough to encompass the actual thermally affected region throughout the transient process. However, it is of interest to avoid the proposition of eigenfunction expansions with variable eigenvalues along the longitudinal coordinate and the time variable. Therefore, we introduce a domain regularization transformation for the spatial domain written as:

$$\eta_{\mathrm{t}} = \frac{y}{\delta_{\mathrm{t}}(x)} \qquad \text{and} \qquad \chi = x \tag{8}$$

The dimensionless form for the fluid energy equation after the domain transformation is given by:

$$\delta_{\mathrm{t}}^2(\chi) \frac{\partial \theta_{\mathrm{f}}(\chi,\eta_{\mathrm{t}},\tau)}{\partial \tau} + \hat{U} \frac{\partial \theta_{\mathrm{f}}(\chi,\eta_{\mathrm{t}},\tau)}{\partial \chi} + \hat{V} \frac{\partial \theta_{\mathrm{f}}(\chi,\eta_{\mathrm{t}},\tau)}{\partial \eta_{\mathrm{t}}} = \frac{1}{Pe_{\mathrm{f}}} \frac{\partial^2 \theta_{\mathrm{f}}(\chi,\eta_{\mathrm{t}},\tau)}{\partial \eta_{\mathrm{t}}^2}, \tag{9a}$$
$$0 < \eta_{\mathrm{t}} < 1, \quad 0 < \chi < 1, \quad \tau > 0$$

where

$$\hat{U}(\chi,\eta_t)=U(\chi,\eta_t)\delta_t^{\,2}(\chi) \quad \text{and} \quad \hat{V}(\chi,\eta_t)=\eta_t U(\chi,\eta_t)\delta_t(\chi)\frac{d\delta_t(\chi)}{d\chi}+V(\chi,\eta_t)\delta_t(\chi) \tag{9b}$$

The initial and boundary conditions become:

$$\theta_f(\chi,\eta_t,0)=0, \qquad 0<\eta_t<1, \quad 0<\chi<1 \tag{9c}$$

$$\theta_f(0,\eta_t,\tau)=\theta_\infty(\tau), \qquad 0<\eta_t<1, \quad \tau>0 \tag{9d}$$

$$\theta_f(\chi,1,\tau)=\theta_\infty(\tau), \qquad 0<\chi<1, \quad \tau>0 \tag{9e}$$

$$\left.\frac{\partial\theta_f}{\partial\eta_t}\right|_{\eta_t=0}=\delta_t(\chi)\left\{\frac{2\left[2(3+Bi_e)\theta_f(\chi,0,\tau)-3(2+Bi_e)\theta_{av}(\chi,\tau)+Bi_e\theta_\infty(\tau)\right]}{K.R(4+Bi_e)}-Q_w(\chi,\tau)\right\},\ 0<\chi<1,\ \tau>0 \tag{9f}$$

And the wall energy equation with the respective initial and boundary conditions are given by:

$$\frac{\partial\theta_{av}(\chi,\tau)}{\partial\tau}=\frac{R}{Pe_s}\frac{\partial^2\theta_{av}(\chi,\tau)}{\partial\chi^2}+6\frac{\left[(2+Bi_e)\theta_f(\chi,0,\tau)-2(1+Bi_e)\theta_{av}(\chi,\tau)+Bi_e\theta_\infty(\tau)\right]}{Pe_s.R(4+Bi_e)}, \qquad 0<\chi<1, \quad \tau>0 \tag{10a}$$

$$\theta_{av}(\chi,0)=0, \qquad 0<\chi<1 \tag{10b}$$

$$\left.\frac{\partial\theta_{av}}{\partial\chi}\right|_{\chi=0}=Bi_0(\theta_{av}(0,\tau)-\theta_\infty(\tau)); \quad -\left.\frac{\partial\theta_{av}}{\partial\chi}\right|_{\chi=1}=Bi_L(\theta_{av}(1,\tau)-\theta_\infty(\tau)), \qquad \tau>0 \tag{10c,d}$$

The flow problem is readily solved according to Blasius similarity transformation, which provides the velocity components to feed into the decoupled transient energy equation. For the thermal problem solution, since there is a preferential convective direction aligned with the flow, the integral transformation was chosen to be operated solely in the transversal direction, along which diffusion predominates. However, equations (9) are still not in the most convenient form for integral transformation, since the boundary condition at the interface involves a non-homogeneous term. A filtering solution is then proposed, so as to eliminate the non-homogeneous boundary condition, in the form:

$$\theta_f(\chi,\eta_t,\tau)=\hat{\theta}_f(\chi,\eta_t,\tau)+F(\eta_t;\chi,\tau) \tag{11}$$

As in (Naveira et al., 2008), a straightforward second degree polynomial filter is proposed, $F(\eta_t;\chi,\tau)$, where χ and τ become parameters of the solution. The filter is obtained from satisfaction of the following three boundary conditions at the transversal domain edges:

$$F(\eta_t;\chi,\tau)=e_0(\chi,\tau)+e_1(\chi,\tau)\eta_t+e_2(\chi,\tau)\eta_t^{\,2}, \qquad 0<\chi<1, \quad 0<\eta_t<1, \quad \tau>0 \tag{12a}$$

$$F(1;\chi,\tau)=\theta_\infty(\tau) \qquad \left.\frac{dF}{d\eta_t}\right|_{\eta_t=1}=0 \tag{12b,c}$$

$$\left.\frac{dF}{d\eta_t}\right|_{\eta_t=0}=\delta_t(\chi)\left\{\frac{2\left[2(3+Bi_e)F(0;\chi,\tau)-3(2+Bi_e)\theta_{av}(\chi,\tau)+Bi_e\theta_\infty(\tau)\right]}{K.R(4+Bi_e)}-Q_w(\chi,\tau)\right\} \tag{12d}$$

Thus, applying the proposed filtering solution to eqs.(9), the resulting filtered problem is given by:

$$\delta_t^{\,2}(\chi)\frac{\partial\hat{\theta}_f(\chi,\eta_t,\tau)}{\partial\tau}+\hat{U}\frac{\partial\hat{\theta}_f(\chi,\eta_t,\tau)}{\partial\chi}+\hat{V}\frac{\partial\hat{\theta}_f(\chi,\eta_t,\tau)}{\partial\eta_t}=\frac{1}{Pe_f}\frac{\partial^2\hat{\theta}_f(\chi,\eta_t,\tau)}{\partial\eta_t^{\,2}}+G(\chi,\eta_t,\tau), \qquad 0<\eta_t<1, \quad 0<\chi<1, \quad \tau>0 \tag{13a}$$

where

$$G(\chi,\eta_t,\tau) = -\delta_t^{2}(\chi)\frac{\partial F(\eta_t;\chi,\tau)}{\partial \tau} - \hat{U}\frac{\partial F(\eta_t;\chi,\tau)}{\partial \chi} - \hat{V}\frac{\partial F(\eta_t;\chi,\tau)}{\partial \eta_t} + \frac{1}{Pe_f}\frac{\partial^2 F(\eta_t;\chi,\tau)}{\partial \eta_t^{2}} \tag{13b}$$

with initial and boundary conditions:

$$\hat{\theta}_f(\chi,\eta_t,0) = -F(\eta_t;\chi,0), \qquad 0<\chi<1, \quad 0<\eta_t<1 \tag{13c}$$

$$\hat{\theta}_f(0,\eta_t,\tau) = -F(\eta_t;0,\tau), \qquad 0<\eta_t<1, \quad \tau>0 \tag{13d}$$

$$\left.\frac{\partial \hat{\theta}_f}{\partial \eta_t}\right|_{\eta_t=0} = \frac{2\delta_t(\chi)\left[2(3+Bi_e)\hat{\theta}_f(\chi,0,\tau)\right]}{K.R(4+Bi_e)}, \quad \text{and} \quad \hat{\theta}_f(\chi,1,\tau)=0, \qquad 0<\chi<1, \quad \tau>0 \tag{13e,f}$$

The wall energy equation, eq.(10a), is also modified to incorporate the proposed filtering solution, eq.(11).

Proceeding with application of the Generalized Integral Transform Technique, the proposed auxiliary eigenvalue problem is written as:

$$\begin{aligned} &\frac{d^2\psi(\eta_t)}{d\eta_t^2} + \mu^2\psi(\eta_t) = 0, && 0<\eta_t<1 \\ &\left.\frac{d\psi}{d\eta_t}\right|_{\eta_t=0} = 0 && \psi(1)=0, \end{aligned} \tag{14a-c}$$

which is readily solved to yield eigenfunctions, eigenvalues, norms, and normalized eigenfuntions, respectively, as:

$$\begin{aligned} &\psi_i(\eta_t) = Cos[\eta_t\mu_i], \qquad 0<\eta_t<1, \qquad i=1,2,... \\ &\mu_i = \frac{(2i-1)\pi}{2}, \quad i=1,2,... \qquad N_i = \int_0^1 \psi_i(\eta_t)\psi_i(\eta_t)d\eta_t = 1/2 \\ &\tilde{\psi}_i(\eta_t) = \frac{\psi_i(\eta_t)}{N_i^{1/2}} = \sqrt{2}Cos[\eta_t\mu_i], \qquad 0<\eta_t<1, \qquad i=1,2,... \end{aligned} \tag{15a-d}$$

The eigenvalue problem (14) allows definition of the following transform-inverse pair:

$$\bar{\hat{\theta}}_{f,j}(\chi,\tau) = \int_0^1 \tilde{\psi}_j(\eta_t)\hat{\theta}_f(\chi,\eta_t,\tau)\mathrm{d}\eta_t \qquad \rightarrow \quad \text{Transform} \tag{16a}$$

$$\hat{\theta}_f(\chi,\eta_t,\tau) = \sum_{j=1}^{\infty}\tilde{\psi}_j(\eta_t)\bar{\hat{\theta}}_{f,j}(\chi,\tau) \qquad \rightarrow \quad \text{Inverse} \tag{16b}$$

Applying the operator $\int_0^1 \tilde{\psi}_i(\eta_t)\_\_\_\_\_ d\eta_t$ over eq.(13a), followed by the inverse formula, then results:

$$\delta_t^{2}(\chi)\frac{\partial \bar{\hat{\theta}}_{f,i}(\chi,\tau)}{\partial \tau} + \sum_{j=1}^{\infty}\left[a_{ij}(\chi)\frac{\partial \bar{\hat{\theta}}_{f,j}(\chi,\tau)}{\partial \chi} + b_{ij}(\chi)\bar{\hat{\theta}}_{f,j}(\chi,\tau)\right] = \bar{g}_i(\chi,\tau), \quad 0<\chi<1, \ \tau>0, \ i=1,2,... \tag{17a}$$

$$\bar{\hat{\theta}}_{f,i}(\chi,0) = -\int_0^1 \tilde{\psi}_i(\eta_t)F(\eta_t;\chi,0)d\eta_t \qquad \text{and} \qquad \bar{\hat{\theta}}_{f,i}(0,\tau) = -\int_0^1 \tilde{\psi}_i(\eta_t)F(\eta_t;0,\tau)d\eta_t \tag{17b,c}$$

$$a_{ij}(\chi) = \int_0^1 \hat{U}(\chi,\eta_t)\tilde{\psi}_i(\eta_t)\tilde{\psi}_j(\eta_t)d\eta_t = \delta_t^2(\chi)\int_0^1 U(\eta_t)\tilde{\psi}_i(\eta_t)\tilde{\psi}_j(\eta_t)d\eta_t \tag{17d}$$

$$b_{ij}(\chi) = \frac{4\delta_t(\chi)\left[2(3+Bi_e)\right]}{K.R(4+Bi_e)} + \frac{1}{Pe_f}\mu_j^2\delta_{ij} + \int_0^1 \hat{V}(\chi,\eta_t)\tilde{\psi}_i(\eta_t)\frac{d\tilde{\psi}_j(\eta_t)}{d\eta_t}d\eta_t \tag{17e}$$

$$\begin{aligned}\overline{g_i}(\chi) = &-\int_0^1 \tilde{\psi}_i(\eta_t)\delta_t^2(\chi)\frac{\partial F(\eta_t;\chi,\tau)}{\partial\tau}d\eta_t - \int_0^1 \tilde{\psi}_i(\eta_t)\hat{U}\frac{\partial F(\eta_t;\chi,\tau)}{\partial\chi}d\eta_t - \\ &-\int_0^1 \tilde{\psi}_i(\eta_t)\hat{V}\frac{\partial F(\eta_t;\chi,\tau)}{\partial\eta_t}d\eta_t + \int_0^1 \tilde{\psi}_i(\eta_t)\frac{1}{Pe_f}\frac{\partial^2 F(\eta_t;\chi,\tau)}{\partial\eta_t^2}d\eta_t\end{aligned} \tag{17f}$$

The wall heat transfer problem can then be described by the partial differential equation (10a) coupled to the transformed fluid temperature fields. Equations (17) and (10) form an infinite coupled system of one-dimensional partial differential equations for the fluid transformed potentials and the wall average temperature. For computational purposes this system is truncated to a sufficiently large finite order, *N*, for the required convergence control. Once the transformed potentials are numerically computed, the inversion formula, eq.(16b), is employed to reconstruct the filtered potentials, in explicit form in the transversal coordinate, and after adding the filtering solution, $F(\eta_t;\chi,\tau)$, the dimensionless temperature distribution, $\theta_f(\chi,\eta_t,\tau)$, is recovered everywhere within the boundary layer and along the transient process. The PDE system is then numerically handled by routine *NDSolve* of the *Mathematica v.5.2* system (Wolfram, 2005).

3. EXPERIMENTAL PROCEDURE

An experimental set-up was assembled for the measurement by an infrared camera of both temporal and spatial evolutions of the temperature on the front surface of a 330x250 mm² black PVC plate (Figure 1). The plate (1) was heated by two flash lamps that have been placed normally to its front face. The plate is maintained vertically at the outlet of a rectangular channel, with 300x250 cross flow section (2). The plate contains multilayer fluxmeters, for the incident heat flux measurements The airflow, generated by a double aspiration fan (3), was directed via a flow calming section in the channel with 700 mm in straight length. This channel allows the airflow to be parallel to the plate and covering the entire of its width. An AC converter voltage (4) controls the fan. The flow velocity associated with each voltage used in the tests was preliminary measured by a propeller anemometer on the outlet section of the channel.

Cartographies of temperature distribution had been obtained by a short-wave infrared camera (5). For recording the infrared frames, the camera was connected to the digital interface box (6). A cable connects the interface box to a break out box, from which a second cable is connected to the PCMCIA card interface mounted on a station (7). The proprietary software allows recording infrared images with 50 Hz sample rate.

The transient process is generated by a sudden supply of the luminous energy, with a fixed duration, given by two halogen lamps (8) on the front face of the plate. The pulse duration was controlled by an electronic timer (9), and could be fixed in the range 0.1 second – 5 hours with an accuracy of 0.02 second. The analysis of Infrared images allows the calculation of the induced elevation of the temperature at each fixed point on the front surface of the plate.

The described set-up was designed in the Laboratory UTAP-Thermomécanique, Université de Reims, for the specific purpose of convection heat transfer investigations. It allows a certain degree of flexibility to adapt the system to a range of different problems such as conjugated heat transfer or cooling of electronic cards.

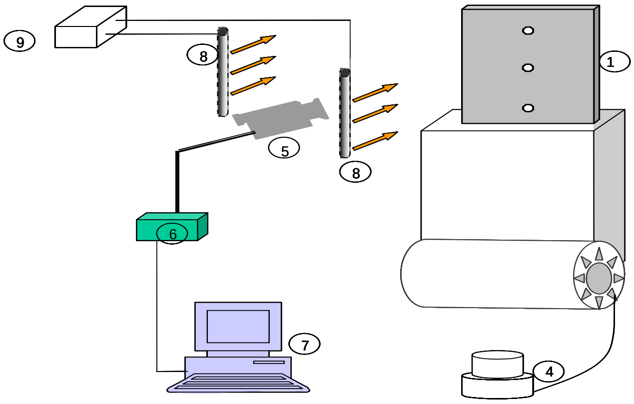

Figure 1 : Experimental setup for conjugated convection-conduction analysis

4. RESULTS AND DISCUSSION

The experimental configuration considered in the present analysis, adopts a black PVC plate of 33 cm in height, thickness of 12 mm and 25 cm wide. The configuration was aimed at insulating the PVC plate within a Styrofoam assembly of 8cm in thickness at the back face and 3.8 cm at the lateral faces. The flash lamps are maintained continuously heating the plate at the same power level.

The thermophysical properties of the black PVC were measured on the Netzsch Nanoflash LFA 447/1 available in the Laboratory of Heat Transmission and Technology (LTTC/COPPE/UFRJ). The LFA 447/1 is a tabletop instrument that works with a high power Xenon-Flash lamp in the temperature range of room temperature to 200°C, and it has an integrated sample changer for 4 samples. The LFA 447/1 is capable of measuring thermal diffusivity in the range of 0.01 mm^2/s up to 1000 mm^2/s, with an accuracy of 3-5% for most materials. The specific heat accuracy is 5-7%. This allows the calculation of the thermal conductivity in the range of 0.1 W/mK 2000 W/mK with an accuracy of 3-7% for most materials (Pinto et al., 2006). The analysis of experimental data was performed with a software called Proteus, provided by Netzsch, providing the following thermophysical properties estimates at 25 C: α=0.144 mm^2/s, k=0.164 W/mC, and c_p=798 J/kgC.

Thermograms were constructed for the transient evolution of the front face temperatures, such as shown in Figure 2, here for the case of an imposed interface heat flux of ϕ=428 W/m^2 starting at t=480s. Also, temperature measurements at the back face of the plate and insulating material were registered to allow estimation of the heat losses. For this situation of an insulated plate, an effective heat transfer coefficient representing the heat losses through the insulating material on the back face was estimated as h_e =2.4 W/m^2C, while at the trailing edge the estimated value is given by h_L =1.6 W/m^2C. The heat transfer at the leading edge has been neglected (h_0 =0). However, since there is a significant uncertainty in such estimated heat transfer coefficients, especially at the back face, due to their variability with time and space, the simulations were performed with both the estimated value and the perfectly insulated assumption(h_e=h_0=h_L=0). Also, one may see from Figure 2 that the free stream temperature is fairly variable along the heating process, and thus it should be considered in the model. Therefore, Figures 3 present a comparison of the experimental (red curve) and theoretical results (black and green curves) for the temperature evolutions at the plate front face, for the selected positions x=11.3, 17.6, 21.1, and 28.3 cm. In general, the set of results for the estimated effective heat losses (black curves) presents a fairly reasonable agreement against the experimental results (red curves), with improved adherence for larger *x* positions along the plate and towards larger time values. On the other hand, the perfectly insulated case (green curves) provides an upper limit for the front face temperature predictions, which aid in encapsulating the experimental results. Clearly, the perfectly insulated case overestimates the front face temperatures at the larger time values, and the crossing of the two curves indicates that the constant heat transfer coefficient along the whole transient process might not adequately model such heat losses, especially at the plate back face, which actually controls the losses by providing a fairly large exchange surface. The nonuniformity of the heat transfer coefficient along the plate height also influences the deviations of experimental and theoretical findings, with the improved agreement for larger values of x. Figure 4.a, on the other hand, provides an indication that the assumption of a constant free stream temperature would have led to underestimated front face temperatures along the whole plate length, especially for the steady-state situation here approached with t=18600 sec, by showing both theoretical results (T_∞=const. in green and $T_\infty(t)$ in black) compared against the experimental results (red curve). Figure 4.b, also compares the steady-state results, but for the cases of estimated heat losses and idealized insulated plate, encapsulating the experiment. Figures 4 also show that there exists significant flow recirculation around the leading edge of the plate, due to the positioning of the plate within the air stream, and that some improvement on this flow arrangement is required for a more adequate comparison of the heat transfer results from the present boundary layer modeling, especially for regions close to the plate leading edge. Such results in part explain the lower temperature values attained by the boundary layer theoretical analysis for lower values of the longitudinal position x.

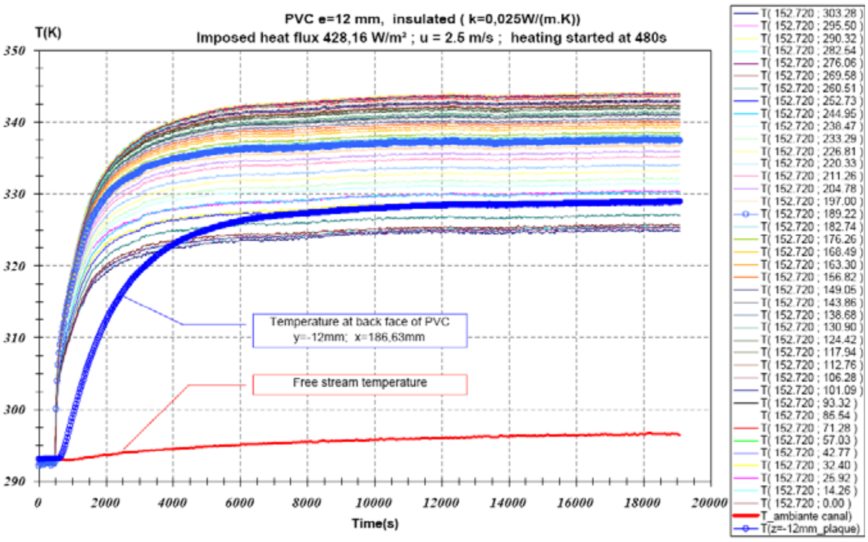

Figure 2 : Thermograms of acquired temperature evolutions with infrared camera (black PVC plate, e=12 mm, ϕ=428.16 W/m^2, u_∞=2.5 m/s, insulated back and lateral faces).

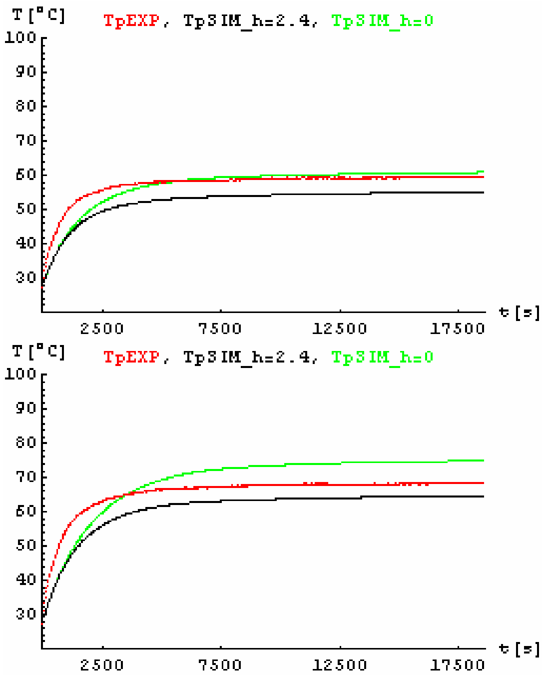

Figures 3: Comparison of transient behavior of front face temperatures along the plate height (x=11.3, 17.6, 21.1, and 28.3 cm), theoretical (green for insulated, and black with heat losses) and experimental (red).

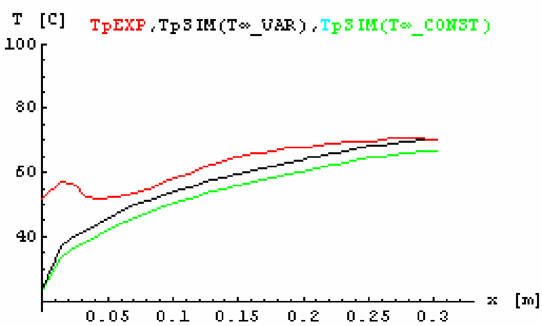

Figure 4.a: Comparison of steady-state temperature distributions, from experiments (red), model with T_∞=const. (green) and T_∞(t) (black). h_e=2.4 W/m^{2}C and h_L=1.6 W/m^{2}C

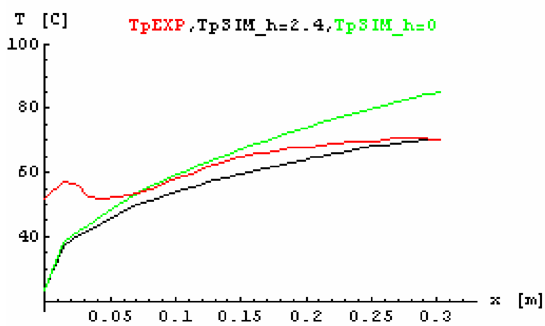

Figure 4.b: Comparison of steady-state temperature distributions, from experiments (red), model with T_∞(t) and insulated plate (green) and heat losses with h_e=2.4 W/m^{2}C and h_L=1.6 W/m^{2}C (black)

5. ACKNOWLEDGEMENTS

The authors (CPN and RMC) would like to acknowledge the kind hospitality of the Laboratoire de Thermomécanique, Université de Reims, France, during their stay in January-February 2008, and would like to acknowledge the financial support provided by CNPq, Brasil and CNRS, France.

6. REFERENCES

Cotta, R.M., 1993, *Integral Transforms in Computational Heat and Fluid Flow*, CRC Press, Boca Raton, Florida, USA.

Cotta, R.M. and Mikhailov, M.D., 1997, "*Heat Conduction: Lumped Analysis, Integral Transforms, Symbolic Computation*", Wiley-Interscience, NY.

Cotta, R.M., Ed., 1998, *The Integral Transform Method in Thermal and Fluids Sciences and Engineering*, Begell House, New York, USA.

Cotta, R. M. and Mikhailov, M.D., 2006, "Hybrid Methods and Symbolic Computations", in: *Handbook of Numerical Heat Transfer*, 2nd edition, Chapter 16, Eds. W.J. Minkowycz, E.M. Sparrow, and J.Y. Murthy, John Wiley, New York, pp.493-522.

Cotta, R.M., Mikhailov, M.D., and Ozisik, M.N., 1987, "Transient Conjugated Forced Convection in Ducts with Periodically Varying Inlet Temperature", *Int J. Heat & Mass Transfer,* V. 30, Nº 10, pp. 2073-2082.

Guedes, R.O.C., Cotta, R.M., and Brum, N.C.L., 1991, "Heat Transfer in Laminar Tube Flow with Wall Axial Conduction Effects", *J. Thermophysics & Heat Transfer*, vol. 5, no. 4, pp. 508-513.

Guedes, R.O.C., and Cotta, R.M., 1991, "Periodic Laminar Forced Convection Within Ducts Including Wall Heat Conduction Effects", *Int. J. Eng. Science*, vol. 29, no. 5, pp. 535-547.

Guedes, R.O.C., Cotta, R.M., and Özisik, M.N., 1994, "Conjugated Periodic Turbulent Forced Convection in a Parallel Plate Channel", *J. Heat Transfer,* vol.116, pp. 40-46.

Lachi, M., Rebay, M., Mladin, E., and Padet, J., 2003, Integral Approach of the Transient Coupled Heat Transfer over a Plate Exposed to a Variation in the Input Heat Flux, *ICHMT Int. Symp. Transient Convective Heat and Mass Transfer in Single & Two-Phase Flows*, August, Cesme, Turkey.

Lachi, M., Cotta, R.M., Naveira, C.P., and Padet, J., 2006, "Improved Lumped-Differential Formulation of Transient Conjugated Conduction-Convection in External Flow", *11th Brazilian Congress of Thermal Sciences and Engineering, ENCIT 2006,* Curitiba, Brasil, Paper no. CIT06-0965, December.

Luikov, A.V., Aleksashenko, V.A., and Aleksashenko, A.A., 1971, "Analytical Methods of Solution of Conjugated Problems in Convective Heat Transfer", *Int. Journal of Heat and Mass Transfer,* vol. 14, pp. 1047-1056.

Luikov, A.V., 1974, "Conjugate Convective Heat Transfer Problems", *Int.J. Heat & Mass Transfer,* vol.17, pp.257-265.

Minkowycz, W.J., Sparrow, E.M., and Murthy, J.Y., Eds., 2006, *Handbook of Numerical Heat Transfer,* 2nd edition, John Wiley, New York.

Mossad, M., 1999, "Laminar Forced Convection Conjugate Heat Transfer over a Flat Plate", *Heat and Mass Transfer,* vol.35, pp 371-375.

Naveira, C.P., Cotta, R. M., Lachi, M., and Padet, J., 2007, "Transient Conjugated Conduction-External Convection with Front Face Imposed Wall Heat Flux", *Proceedings of IMECE2007, ASME International Mechanical Engineering Congress & Exposition,* Paper no. IMECE2007-41417, Seattle, Washington, USA, November 11-15.

Naveira, C.P., Lachi, M., Cotta, R. M., and Padet, J., 2008, "Hybrid Formulation and Solution for Transient Conjugated Conduction-External Convection", *Int. J. Heat & Mass Transfer,* in press

Perelman, Y.L., 1961, "On Conjugate Problems of Heat Transfer", *Int. J. Heat and Mass Transfer*, vol. 3, pp.293-303.

Pinto, C.S.C., Massard, H., Couto, P., Orlande, H.R.B., Cotta, R.M., and Ambrosio, M.C.R., 2006, "Measurement of Thermophysical Properties of Ceramics by the Flash Method", METROSUL IV, 4th Congresso Latino-Americano de Metrologia**,** Foz do Iguaçú, November 2004;also, *Brazilian Archives of Biology and Technology,* V.48, pp.31-39.

Pozzi, A. and Tognaccini, R., 2000, "Coupling of Conduction and Convection past an Impulsively Started Semi-infinite Flat Plate", *Int. J. of Heat and Mass Transfer*, vol. 43, pp. 1121-1131.

Rebay, M., Lachi, M., and Padet, J., 2002, Mesure de coefficients de convection par méthode impulsionnelle—influence de la perturbation de la couche limite, *Int. J. of Thermal Sciences,* vol. 41, pp.1161–1175.

Rebay, M., Mladin, E., Chemin, S., and Stoian, M., 2008, "Dissipative Fluxmeter for the Validation of the Heat Transfer Coefficient Measurement by the Pulsed Method", *Eurotherm 2008,* Eindhoven, Netherlands, June.

Remy, M., Degiovanni, A., and Maillet, D., 1995, Mesure de coefficient d'échange pour des écoulements à faible vitesse, *Rev. Gén. Therm***.** vol.397, pp.28–42.

Santos, C.A.C., Quaresma, J.N.N., and Lima, J.A., 2001, *Benchmark Results for Convective Heat Transfer in Ducts: - The Integral Transform Approach*, ABCM Mechanical Sciences Series, Ed. E-Papers, Rio de Janeiro.

Vynnycky, M., Kimura, S., Kanev, K., and Pop, I., 1998, "Forced Convection Heat Transfer from a Flat Plate: The Conjugate Problem", *Int. J. of Heat and Mass Transfer*, vol.41, pp. 45-59.

Wolfram, S., 2005, *The Mathematica Book*, version 5.2, Cambridge-Wolfram Media.

7. RESPONSIBILITY NOTICE

The authors are the only responsible for the printed material included in this paper.